Ann. Geophys., 30, 389–404, 2012
www.ann-geophys.net/30/389/2012/
doi:10.5194/angeo-30-389-2012

Annales Geophysicae

Revisiting "Narrow Bipolar Event" intracloud lightning using the FORTE satellite

A. R. Jacobson[1] **and T. E. L. Light**[2]

[1]Earth and Space Sciences Department, University of Washington, Seattle, WA, USA
[2]ISR2, Los Alamos National Laboratory, Los Alamos, NM, USA

Correspondence to: A. R. Jacobson (abramj@u.washington.edu)

Received: 11 November 2011 – Revised: 14 February 2012 – Accepted: 15 February 2012 – Published: 24 February 2012

Abstract. The lightning stroke called a "Narrow Bipolar Event", or NBE, is an intracloud discharge responsible for significant charge redistribution. The NBE occurs within 10–20 µs, and some associated process emits irregular bursts of intense radio noise, fading at shorter timescales, sporadically during the charge transfer. In previous reports, the NBE has been inferred to be quite different from other forms of lightning strokes, in two ways: First, the NBE has been inferred to be relatively dark (non-luminous) compared to other lightning strokes. Second, the NBE has been inferred to be isolated within the storm, usually not participating in flashes, but when it is in a flash, the NBE has been inferred to be the flash initiator. These two inferences have sufficiently stark implications for NBE physics that they should be subjected to further independent test, with improved statistics. We attempt such a test with both optical and radio data from the FORTE satellite, and with lightning-stroke data from the Los Alamos Sferic Array.

We show rigorously that by the metric of triggering the PDD optical photometer aboard the FORTE satellite, NBE discharges are indeed less luminous than ordinary lightning. Referred to an effective isotropic emitter at the cloud top, NBE light output is inferred to be less than $\sim 3 \times 10^8$ W.

To address isolation of NBEs, we first expand the pool of geolocated intracloud radio recordings, by borrowing geolocations from either the same flash's or the same storm's other recordings. In this manner we generate a pool of $\sim 2 \times 10^5$ unique and independent FORTE intracloud radio recordings, whose slant range from the satellite can be inferred. We then use this slant range to calculate the Effective Radiated Power (ERP) at the radio source, in the passband 26–49 MHz. Stratifying the radio recordings by ERP into eight bins, from a lowest bin (<5 kW) to a highest bin (>140 kW), we document a trend for the radio recordings to become more isolated in time as the ERP increases. The highest ERP bin corresponds to the intracloud emissions associated with NBEs. At the highest ERP, the only significant probability of temporal neighbors is during times following the high-ERP events. In other words, when participating in a flash, the high-ERP emissions occur at the apparent flash initiation.

Keywords. Meteorology and atmospheric dynamics (Atmospheric electricity; Lightning)

1 Introduction

1.1 Background

The name "Narrow Bipolar Event" refers to a particular, perhaps distinctive Very Low Frequency (VLF; 3–30 kHz) and Low Frequency (LF; 30–300 kHz) signal radiated by intracloud lightning. It was first described over thirty years ago (Le Vine, 1980). Two observables were interrelated: the first observable was the VLF/LF signal (called a "sferic" in common with the VLF/LF radiated signatures of all large-scale lightning strokes). The second observable was extremely intense superimposed noise at High Frequency (HF, 3–30 MHz) and Very High Frequency (VHF, 30–300 MHz). The latter was conveyed by Le Vine's article's title, "Sources of the strongest rf radiation from lightning". Since then the name Narrow Bipolar Event, or NBE, has been used (with some license) to refer not only to the sferic, but also to the intense radiation at higher frequencies. The NBE resembles a single full cycle of a distorted sine-wave, with a risetime of 1–2 µs, then falling and crossing zero in a few microsec, followed by the second half-cycle, which is lower-amplitude but longer-duration compared to the first half-cycle. The typical NBE full-width is 10–20 µs, which is less than most (though not all) negative cloud-to-ground sferic waveforms (Willett et al., 1990, 1998; Willett and Krider, 2000). The name "NBE" has sometimes been replaced by "Compact

Intracloud Discharge", or CID (e.g., Nag et al., 2010), but both monikers refer to the same set of observables. The present report will continue to use the earlier term "NBE", despite its defects.

It has been inferred since the outset that NBEs had an intracloud origin (Willett et al., 1989). The extremely intense VHF radiation associated with NBEs made it possible for a satellite-borne radio recorder (Holden et al., 1995) to trigger and record this phenomenon from orbit, with the Blackbeard payload aboard the Alexis satellite. Blackbeard, which was designed, built, and integrated into the satellite under the leadership of T. Armstrong (deceased), had a simple amplitude trigger, and thus was relatively poorly suited to triggering off of lightning impulses amongst the confusing background of man-made radio-communications carriers. Nonetheless, the exceptional intensity of the NBE emissions at VHF allowed these events to cause triggers and to be recorded by Blackbeard. Unlike the ground-based measurements from the 1980s, the Blackbeard recordings showed a characteristic pair of noise bursts, separated by tens of microseconds (Holden et al., 1995). These pairs were interpreted as being due to propagation along two paths to the satellite, the first being the direct path, and the second being a ground-reflected path (Massey and Holden, 1995; Massey et al., 1998a; Zuelsdorf et al., 1997, 1998). The pairs were named "Transionospheric Pulse Pairs", or TIPPs for short. This acronym is based purely on the appearance of the VHF pulse recorded on a satellite above the ionosphere. In the remainder of this article, we will use the word TIPP to apply to satellite-recorded VHF signals containing a distinct double pulse which indicates an elevated intracloud source.

A possible objection to the ground-reflection model of TIPPs would be that the second pulse is sometimes stronger than the first, implying a reflected wave that is stronger than the incident wave. Of course, with a linearly-polarized dipole emitter, this is perfectly feasible and expected (Tierney et al., 2002). Moreover, it was shown by direct experiment that the effective reflectivity of dry, flat ground at a frequency passband near 100 MHz was high enough to account for TIPPs (Massey et al., 1998a). This demonstration was done with an Electromagnetic Pulse (EMP) generator flown on a balloon payload 2.6 km above the ground in the White Sands Missile Range. Receivers on towers about 20 m above the ground were able to record both the incident and the reflected pulses from the EMP generator, while the balloon was at 23-deg elevation angle. The authors found the energy reflection coefficient to be 0.94 ± 0.06 for horizontal polarization and 0.78 ± 0.09 for vertical polarization. The soil at White Sands was characterized as dry and alkaline. They concluded from this balloon experiment that the second pulse in Blackbeard TIPPs could feasibly be a ground reflection.

Very soon after the Blackbeard satellite reports, a collaboration of Langmuir Laboratory for Atmospheric Research and Los Alamos National Laboratory discovered an innovative way to determine the height of the NBE source from the sferic waveform (Smith, 1998; Smith et al., 1999). They used a capacitive antenna originally developed by M. Brook at Langmuir for studying fast transients in the vertical electric field ("fast E-field changes"), i.e., sferics in the VLF/LF spectrum (Kitagawa and Brook, 1960). Some of the NBE sferics were followed by a distinctive pair of secondary echoes, delayed by as much as a few-hundred microsec from the initial ground-wave signal. It was noted that this double-echo pattern is precisely what what would be expected of a delayed ionosphere reflection followed by an even more delayed ground reflection plus ionosphere reflection (Smith, 1998; Smith et al., 1999). If one knows the horizontal range to the sferic source (through multi-station differential time of arrival) then the two echoes' delays can be used to solve for the virtual height H_i of the ionospheric reflector and the height of the source, H_s. On the other hand, if one has only a single-sensor recording of the sferic, and the horizontal location is unkown, one can still retrieve the approximate range to the sferic and the approximate source height, assuming H_i to be around 85 km during night and around 70 km during day. This innovation in using the NBE sferic's delayed echoes allowed the vertical source distribution to be studied (Smith et al., 1999, 2004). It was found that the source always occured at intracloud-lightning heights (7–14 km, and occasionally up to 18 km).

An even more significant finding from M. Brook and his colleagues at Langmuir Laboratory was a clear association of the NBE sferics with radar echoes of thunderstorms, although publication of this result awaited the Langmuir-Los Alamos collaboration (Smith, 1998; Smith et al., 1999).

A development from the Langmuir/Los Alamos collaboration was the Los Alamos Sferic Array, which recorded sferic waveforms and provided time-of-arrival location of sferic sources, always with the Brook antenna design. By 1998, LASA covered sferics in much of the southern Great Plains and New Mexico (Massey et al., 1999), and by 1999 LASA was expanded to include a denser subarray in Florida (Smith et al., 2002).

At about the same time as the Langmuir/Los Alamos collaboration on the NBE sferic echoes, the FORTE satellite (launched in 1997) was providing triggered recordings of lightning VHF emissions (Jacobson et al., 1999), including, but not limited to, the intense VHF associated with NBEs. FORTE's principal radio-receiver trigger system was based on multi-channel coincidence. This advance with respect to Blackbeard allowed reliable triggering on wideband impulses (like lightning), and was largely immune to false triggers from communication carriers (Jacobson et al., 1999). The double-pulse structure of TIPPs could be used to retrieve the source height for cases where the source's horizontal location was already known (Jacobson et al., 2000), e.g., by coincidence with the National Lightning Detection Network (Cummins et al., 1998). Some FORTE-recorded TIPPs were coincident with LASA NBE sferics. During these simultaneous observations of LASA NBEs and of coincident

FORTE TIPPs, the source heights retrieved by both LASA and FORTE agreed to within $+/-1$ km (Smith et al., 2004).

Further observations on NBEs and their associated VHF TIPPs were presented in publications based on FORTE (Jacobson, 2003a, b; Jacobson and Light, 2003; Light and Jacobson, 2002) and on LASA (Jacobson and Heavner, 2005; Jacobson et al., 2007; Suszcynsky and Heavner, 2003; Wiens et al., 2008). Recently it has been shown that the VHF pulse in the TIPP associated with NBEs is neither polarized nor coherent (Jacobson et al., 2011). Both the directly-propagated VHF pulse and the ground-reflected VHF pulse in an NBE-associated TIPP are individually about 5–15 µs wide, during which the amplitude undergoes many irregular fades.

FORTE carried an optical photometer to measure the light output from lightning discharges. Perhaps the most noteworthy finding of the FORTE project was that the strongest VHF intracloud pulses are accompanied by very little light compared to other lightning process (Light and Jacobson, 2002). Testing this further will be a major goal of the present report.

1.2 Goals of the present study

This article presents new analysis and interpretation of existing FORTE and LASA data, in order better to test two earlier hypotheses about NBEs:

(a) The first hypothesis is that NBEs are far less luminous than are other forms of lightning. If this were true, it would imply that the current (to radiate the sferic) must be carried by some means other than an incandescent plasma channel, e.g., by energetic electrons causing only weak flourescence in the background air. The only other atmospheric-electrification process clearly necessitating energetic electrons is the Terrestrial Gamma-Ray Flash (Dwyer, 2008; Grefenstette et al., 2008, 2009). Given the significance of that implication, the "less-luminous-NBE" hypothesis will be subjected below to a new test that has not previously been performed. The less-luminous-NBE hypothesis (Light and Jacobson, 2002) was based on observing that, for the more intense TIPP records, as the TIPP electric field amplitude at the FORTE VHF antenna increased, the likelihood of coincident triggering by FORTE's PDD photometer (Kirkland et al., 2001) tended to *decrease*. In other words, more-intense VHF was accompanied by less-intense light. Although convincing, this evidence had the drawback that the VHF sources had not been located. The radio field of view for FORTE was out to the Earth's limb (at radius 3000 km from the subsatellite point), while the PDD field of view was out to only a 600-km radius. This was unfortunate for two reasons: first, the radio-contributing area (assuming no drop-off of the detection efficiency with range) was ∼25-fold larger than the optically-contributing area. This meant that the pool of VHF events would, a priori, be less than 4 % likely to have optical concurrence from PDD. Second, a given VHF power flux density at the antenna could represent a source Effective Radiated Power (ERP) varying by an unknown and random factor of ∼17, the lowest implied ERP being for a source at nadir (range ∼800 km) and the largest implied ERP for a source at the limb (slant range ∼3300 km). This tends to blur detection of a trend, if there is such a trend, in optical concurrence versus VHF ERP.

(b) The second hypothesis is that NBEs are relatively isolated in time, compared to other forms of lightning. This was proposed in the first reports of NBEs (Le Vine, 1980; Willett et al., 1989), but was somewhat contradicted by later studies based on the Lightning Mapping Array (Rison et al., 1999; Thomas et al., 2001), which reported NBEs initiating intracloud flashes. Recently, a ground-based study of NBEs (Nag et al., 2010) observed that out of a total of 157 events, 73 % were isolated. A more extensive survey of 11 876 NBEs in China (Wu et al., 2011) finds that neighbors are very improbable (<2 %) in the 10 ms preceding an NBE, but are sometimes seen (∼12 % for positive-polarity NBEs, ∼4 % for negative-polarity NBEs) in the ten millisec following the NBE. This matter has important implication: Without a prior leader process to ionize the air and prepare a conductive channel, how can a large-scale charge transfer (stroke) occur? Given the importance of this issue, we revisit FORTE data to provide better statistics on the flash setting of NBEs.

2 Data resources for this study

The present study is based on simultaneous observations from the following sources:

- The National Lightning Detection Network, or NLDN (Cummins et al., 1998; Cummins and Murphy, 2009).
- The Los Alamos Sferic Array, or LASA (Smith et al., 2002).
- The Photodiode Detector, or PDD, aboard the FORTE satellite (Kirkland et al., 2001).
- The Lightning Location System, or LLS, optical imager aboard the FORTE satellite (Suszcynsky et al., 2001).
- The Very High Frequency, or VHF, radio receivers aboard the FORTE satellite (Jacobson et al., 1999).

(a) Research-grade, stroke-level data from NLDN was used to provide ground truth on lightning strokes for the FORTE satellite, during two warm seasons: April through September 1998 and May through October 1999 (Jacobson et al., 2000). This joint campaign covered the Continental United States (CONUS) with NLDN's high detection efficiency (Cummins et al., 1998). In addition, relaxation of the usual range limit (which would ordinarily reject located strokes more than 625 km from participating sensors) allowed useful detection of some strokes, albeit with diminishing detection efficiency, beyond the ordinary limits of the CONUS. This ground-truth campaign allowed

the unambiguous identification of radio signatures that are characteristic of various stroke types (positive and negative cloud-to-ground, or +CG and −CG; intracloud, or IC; etc.). This ground-truthing by NLDN allowed development of a rudimentary identification of stroke type from the FORTE-recorded radio waveform alone (Suszcynsky et al., 2000).

(b) LASA (Smith et al., 2002) served as a small lightning-location research array complementing the continental-scale NLDN. LASA contained several stations initially in and near New Mexico (during 1998), and then (during 1999–2002) in Florida. LASA's utility to this study is its recording of entire waveforms of "sferics", or transient electric fields from lightning strokes in the spectral region 1 to 300 kHz. These sferics were sampled over several millisec, with a sampling rate of 1 Megasamples/s. These waveform recordings were extremely useful for studying characteristics of lightning discharges, including NBEs (Heavner et al., 2002; Jacobson and Heavner, 2005; Jacobson et al., 2007; Smith et al., 1999, 2004; Suszcynsky and Heavner, 2003). Indeed, the only completely reliable way of identifying a sferic as being due to an NBE is to examine details of its recorded waveform *from several stations*.

(c) The PDD aboard the FORTE satellite used a silicon photodiode with broadband visible/near-infrared response (Kirkland et al., 2001). PDD provided non-imaging lightning detection of strokes within a 600-km-radius circle centered on the satellite nadir. The irradiance versus time was digitized with a 15-µs sampling interval, and individual records could be of variable length, though were most often selected to be 1.9 ms (128 samples) long. In nighttime self-triggered mode (which applies to the data used here), a trigger occurs when the rising edge of an optical pulse exceeds a selected multiple of the background noise (Kirkland et al., 2001). The pretrigger 32 samples and the posttrigger 96 samples constitute the recording, in the most common case of 128 total samples. In ordinary operations, PDD was used only during local night. During this nighttime mode, the effective trigger threshold corresponded to peak optical irradiance (at the satellite, 800 km altitude) around $3.5 \times 10^{-5}\,\mathrm{W\,m^{-2}}$. Taking account of the 825-km altitude of FORTE, we infer that the corresponding peak, isotropic effective radiated power (ERP) would be $\sim 3 \times 10^8$ W. This is the PDD threshold ERP referred to the top of the cloud, not at the location (deeper within the cloud) of the actual discharge. The top of the cloud is the directly-viewed radiant source, because the actual discharge is generally obscured by intervening cloud scattering (Koshak et al., 1994).

(d) The LLS optical imager (Suszcynsky et al., 2001) was based upon H. Christian's successful CCD design (Christian et al., 2003) employed in both OTD (Boccippio et al., 2000) and LIS (Christian et al., 1999). The LLS field of view was a 600-km × 600-km square, surrounding the PDD field of view. This field of view contained 128 × 128 pixels. The pixel size at nadir was less than 10 km. LLS functioned well during local night, as long as the satellite was outside the South Atlantic Anomaly, within which elevated particle fluxes caused frequent false light detections. The framing temporal resolution of the CCD (2 ms) in LLS is too long to permit close examination of the timing relationship between LLS events and other means of detecting lightning, e.g., sferics and VHF. For studying timing comparisons between light and either sferics or VHF, the PDD is preferable, due to its short (15-µs) sample resolution.

(e) The FORTE VHF radio-receiver and -recording system (Jacobson et al., 1999) used in this study consisted of a pair of channels synchronously sampled at 50 Megasamples/s, with 12 bit digitization. The analog bandwidth was ∼23 MHz, with a low-pass analog filter attenuating the uppermost 2 MHz of the nominal 25-MHz bandwidth. In the data used here, one channel was always in the range 26–49 MHz, while the second channel could be either at 26–49 MHz or at 118–141 MHz, programmably. Typical record lengths were ∼400 µs; for this length, the on-board memory could store over a thousand pairs of recordings. Downlinks occurred several times per day, so that several-thousand radio-emission events per day could be obtained. This particular dual-channel receiver system was in full operation by December 1997; it failed in December 1999, after which FORTE used a single-channel, 85-MHz-bandwidth receiver. More details are available elsewhere (Jacobson et al., 1999, 2000; Jacobson and Shao, 2002; Shao et al., 2004, 2005; Shao and Jacobson, 2001, 2002; Suszcynsky et al., 2000).

3 A direct test of the optical output of narrow bipolar events

The LASA Florida sub-array (Smith et al., 2002) was in full operation from May 1999 through November 2002, locating lightning strokes and storing digitized waveforms for four years of Florida's warm-season thunderstorms. The array contained several receiver stations, and the array's coverage area was centered on −81.5° E, 28.0° N. For strokes lying within a 400-km-radius circle centered on this point, LASA provided reliable locations and digitized waveforms whose details were dominated by the groundwave, as opposed to the ionospheric reflection. This usually allowed straightforward identification of the type of stroke causing the signal (Jacobson and Heavner, 2005; Jacobson et al., 2007; Smith et al., 2002, 2004).

We have identified local-night-time windows during which PDD was armed, programmed to trigger, and with at least some of the LASA 400-km-radius circle within the PDD field of view. We prepared a digital catalogue of those detected/located LASA strokes which (a) occurred within the instantaneous PDD field of view, and (b) occurred during a PDD-armed time window. Applying these criteria narrowed the list of LASA events to just 10 061 strokes, on the order of only 0.1 % of the total of LASA records in Florida.

Figure 1 shows a histogram of the 10 061 LASA event times, minus the time-of-flight-corrected PDD trigger time, for all LASA events within the 400-km circle and simultaneously within the PDD field-of-view during times in which PDD was armed, triggering, and recording. The abscissa is between ±10 ms. The heavy black curve shows the distribution of corrected time differences. Of the 10 061 selected LASA events, only 1651 have a PDD coincidence within ±10 ms. The main peak of the time-difference distribution occurs at ∼ −300 µs, and is several-hundred microsec in width. The estimated uncertainty in timing is due to the two main effects: (a) FORTE timestamping errors, perhaps 10 µs, and (b) FORTE ephemeris errors, slightly larger when translated to time, 20–30 µs. Thus the outer range of errors in timing is ±30 µs, so both the peak location and the peak width in this histogram are physically meaningful, not significantly affected by observational errors. In an earlier report, PDD was correlated with NLDN stroke detections for April–September 1998 (Kirkland et al., 2001). The histogram of time differences in Kirkland et al's Fig. 5 is (apart from a sign change on the abscissa due to definition of time-difference convention) almost identical to the distribution we find (our Fig. 1) for LASA-PDD time differences. The mean shift of the distribution is related to the delay of the light (seen from a satellite) relative to the sferic stroke with which it is correlated. It has been shown that this delay can be partitioned as a sum of "physical delay" and "propagation delay" (Davis et al., 2002; Kirkland et al., 2001; Light et al., 2001a, b; Suszcynsky et al., 2000). The physical delay is due to the observation that in a cloud-to-ground stroke, for example, the sferic is emitted promptly at the contact of the descending leader with the ground, while the light emission visible to a satellite is delayed until the charge-transfer electrical transient can spread into the upper reaches of the cloud. This is a physical delay for an electrical transient to develop into a region where the emitted photons have a higher chance of being seen by a satellite. On the other hand, the "propagation delay" is due to the diffusion of light outward through intervening cloud before reaching the cloud surface (Koshak et al., 1994; Light et al., 2001b). Each of these types of delay in turn has great variability, so the distribution of sferic-minus-light time differences is not only grossly displaced, but also broadened. The distribution in Fig. 1 is broadly consistent with the picture of delay and time-spreading introduced a decade ago.

In Fig. 1 we mark with vertical green lines the LASA-PDD time differences for events classified by LASA as NBEs. There are 16 such NBEs in ±10 ms relative to the nearest PDD event. Below, we shall show that the five most central of these 16 NBEs are miss-classified and are not really NBEs, but rather, negative cloud-to-ground strokes. However, before doing that, we will show the the small number of (false) NBEs still constitute a rather small portion of NBEs with closely associated PDD activity. We define the region from −800 µs to +200 µs as being the "tightly coincident" core of the histogram. This region is wide enough to capture the peak and its flanks, but narrow enough to exclude most of the accidental coincidences. With this definition, there are 4 NBEs that are tight coincidences with PDD, and 1134 non-NBEs that are tightly concident with PDD. The ratio of NBEs/non-NBEs overall is 0.016, while amongst the events tightly coincident with PDD, the ratio is 0.0035. Thus we can state immediately: If an NBE occurs, that NBE is less than 25 % as likely, relative to a non-NBE, to be tightly coincident with light detected by PDD. This direct result is consistent with what had been inferred earlier from more circumstantial evidence, namely that NBEs are a relatively "dark" process (Light and Jacobson, 2002).

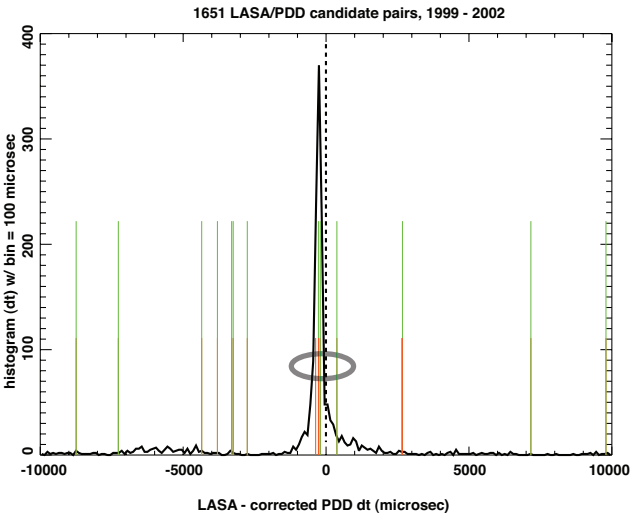

Fig. 1. Histogram of time difference of LASA sferic, minus the time-of-flight-corrected PDD optical photometer trigger time. The binsize is 100 µs. There are 10 061 LASA sferics located within the instantaneous PDD field-of-view during PDD nighttime operation. Of these, 1651 sferics occur within ±10 ms of a PDD trigger, and their time distribution relative to the PDD trigger is shown by the black curve. This distribution peaks at −300 µs. We define "tight coincidence" to mean a sferic/PDD pair whose LASA-PDD time difference lies in the range −800 to +200 µs, which is centered on −300 µs. Vertical green lines mark the 16 cases of an NBE sferic being within ±10 ms of a PDD trigger, and the sferic waveforms are archived. Red vertical lines indicate cases where the sferic waveforms are not available for all of the stations. The grey ellipse marks five apparent NBE/PDD coincidences, four of them within the tight-coincidence window, and the fifth just outside that window but still meriting further attention.

This matter of NBEs behaving as "dark lightning" (relative to other lightning) is sufficiently contentious, as well as sufficiently puzzling, that we return to the data of Fig. 1 and examine in detail the tight-coincidence events classified by LASA as NBEs. The ellipse in Fig. 1 marks the four tight-coincidence NBEs with $-800 < \mathrm{dt} < +200$ µs, plus an additional event with dt = +378 µs, which is nearby. Table 1 summarizes the statistics of the correlation between LASA and PDD.

Table 1. LASA/PDD joint observations within 400 km radius of array center.

Date range of LASA/PDD joint observations	1 May 1999 to 17 Nov 2002
Geographic range of candidate LASA events	within 400-km-radius from 28° N, −81.5° E
# of LASA events without PDD in ±10 ms (null)	8410
# of LASA events with PDD in ±10 ms	1651
# of LASA NBEs without PDD in ±10 ms (null)	149
# of LASA NBEs with PDD in ±10 ms	16
# of LASA events with PDD in −0.8 to +0.2 ms	1138
# of LASA NBEs with PDD in −0.8 to +0.2 ms	4
ratio of NBEs:non-NBEs, overall	0.016
ratio of NBEs:non-NBEs, with PDD in −0.8 to +0.2 ms	0.0035

Table 2. Sixteen LASA/PDD coincidences within ±10 ms. Boldfaced lines are for the 5 cases of |dt| within the central peak of histogram (dt).

Number	LASA trigger UT yyyymmdd_hh.mm.ss.sss	NBE waveforms stored?	LASA – PDD dt (microsec)
0	20010623_14.00.38.514	yes	−3249
1	**20010623_14.00.51.464**	**yes**	**−266**
2	**20010701_23.13.31.825**	**no, but restored**	**−259**
3	20010809_03.53.01.638	no	2652
4	20010817_02.23.45.476	yes	−3800
5	20010817_02.23.45.476	yes	−8744
6	**20010818_02.01.13.897**	**yes**	**378**
7	**20010826_00.33.54.376**	**yes**	**202**
8	**20010829_10.03.08.293**	**no, but restored**	**−364**
9	20020817_06.18.56.635	yes	−3304
10	20020819_05.30.02.149	yes	7166
11	20020819_05.30.02.149	yes	2673
12	20020826_04.20.31.980	yes	−7268
13	20020826_04.20.34.469	yes	−4352
14	20020826_04.20.56.546	yes	9793
15	20021110_01.26.41.664	yes	−2756

The five events which are included in the ellipse are all classified as NBEs by the original LASA stroke-classifier algorithm (see Smith et al.'s Fig. 14 and Sect. 4, in Smith et al., 2002). This algorithm works by examining two parameters: (1) the sum of the rise-time and fall-time of the initial sferic pulse, and (2) the signal-to-noise ratio of the pulse within its (typically 8-ms) recording length. On the plane defined by these two parameters, Smith et al. observed a clear clustering of data into two distinct swarms, one at high SNR/small width (NBE swarm), and another at low SNR/large width (non-NBE swarm, usually cloud-to-ground strokes). This, and variations of it (Wiens et al., 2008), worked very well in separating NBEs from other sferics such as cloud-to-ground return strokes, with an acceptably small rate of false NBEs. Figure 2 shows the LASA station layout (triangles) and the stroke location (square symbol) for a typical true-classification NBE from 2 June 1999. Figure 3 shows 1024 samples of the digitized electric field at each of the four stations, with shortest range at the top, and longest range at the bottom. Both Fort Myers and Gainesville had high levels of instrumental noise, while Boca Raton and Tampa had cleaner records. The algorithm used Fort Myers for the stroke classification, and not surprisingly, the classification is positive-polarity NBE (Smith et al., 1999, 2002).

The operational algorithm for classifying a stroke as an NBE is based on the ground wave alone, and is implemented on the single station, excluding the closest, having the lowest instrumental-noise contamination. If one is willing to examine multiple-station data simultaneously, tediously by eye, there is a more secure confirmation of the stroke's being an NBE in Fig. 3: The pair of ionospheric echoes (marked "e1", "e2") display the expected trends versus range: they become

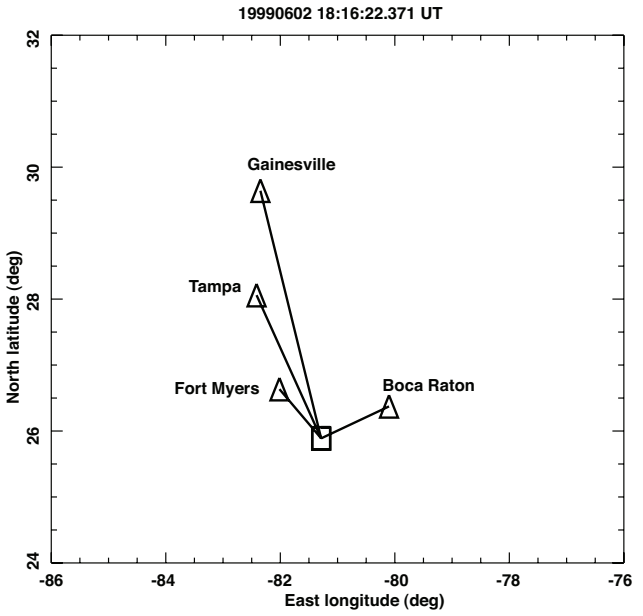

Fig. 2. Map of the four participating LASA stations (triangles) in Florida, connected by baselines (black lines) to the sferic source location (square), for a single example of a Narrow Bipolar pulse. This is a daytime example, when PDD data would not be available, but is meant to show the characteristics of the NBE sferic on recorded at multiple ranges.

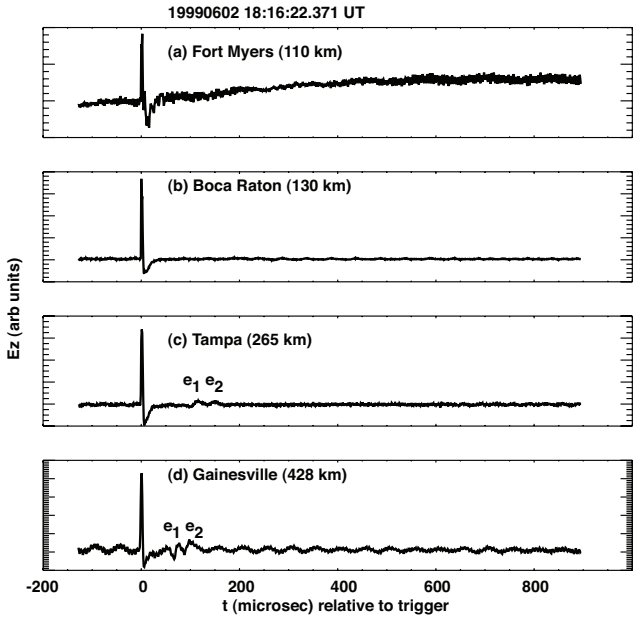

Fig. 3. Vertical electric field versus time (relative to each station's trigger at $t = 0$), for the four LASA stations participating in the solution for the case of Fig. 2 above. The range of each station from the lightning is in parentheses. The Fort Myers station exhibits high-frequency electronic noise, while the Gainesville station has a narrowband noise ripple. The two echoes from the ionosphere are marked, and their relative amplitudes and delays from the ground wave are as is expected due to the reflection geometry. These two features of the echoes – increasing relative amplitude with increasing range, and decreasing delay with increasing range – are both outcomes of the ionospheric reflections process.

larger (relative to the groundwave peak) at longer range, and they recede back toward the groundwave peak at longer range (see Figs. 1–3, and discussion thereof, in Smith et al., 2004). Those two dependencies versus range make it certain that the waveform arises from an elevated discharge, i.e., an intracloud discharge.

Let us now examine the sferic waveforms recorded by LASA for the five events marked in Fig. 1 by an ellipse. Table 2 gives the times of all sixteen cases of strokes classified as NBEs and having PDD correlation within ± 10 ms. Sferic #5 is the same as #4, and #11 is the same as #10. This is due to there being more than one PDD to correlate with, within ± 10 ms of either sferic. The five rows shown with boldface font in Table 2 are for the five events near the central peak (four officially in the peak, and the fifth very near the peak, where the peak is defined as -800 to $+200$ µs).

Figure 4 shows the four electric-field waveforms for row #1 in Table 2. The vertical arrow occurs at the same time in each of the four ranges, and indicates the nominal position of the second "ionospheric echo". Apparently the "ionospheric echoes" (e1, e2) occur at a fixed delay after the principal pulse, rather than recede toward the principal pulse as range increases. Moreover, the amplitudes of the "echoes" relative to the principal pulse do not show either the expected null near zero range nor the expected monotonic growth as range increases. These two facts indicate that this event had been erroneously classified as an NBE using the single-station automated LASA classifier algorithm. In fact it is an exceptionally uncluttered negative cloud-to-ground stroke, such as those used in a recent study of D-region VLF/LF reflection (Lay and Shao, 2011).

Figure 5 is similar to Fig. 4 but for the "NBE" in row #6 of Table 2. In this figure, the vertical arrows are all aligned in time, and mark the nominal location of the first "ionospheric echo". Again for the same reasons, we see that a negative cloud-to-ground stroke had been falsely classified as a negative NBE. Figure 6 repeats this exercise for the case of row #7 of Table 2, and as in the previous two figures, we can deduce that the stroke is negative cloud-to-ground. (Note: the Boca Raton preamplifier had strong self-oscillation; this is non-physical.)

The waveforms for the above three cases (Figs. 4, 5, and 6) had been completely archived. Table 2 shows two cases of a partial loss of multi-station NBE waveform data, although it is possible to restore at least one station's data in each case. Figure 7 shows the one station's waveform for (a) row #2 of Table 2, and (b) row #8 of Table 2. Both of these cases are obviously negative cloud-to-ground, despite their having been classified as negative NBE by the original algorithm.

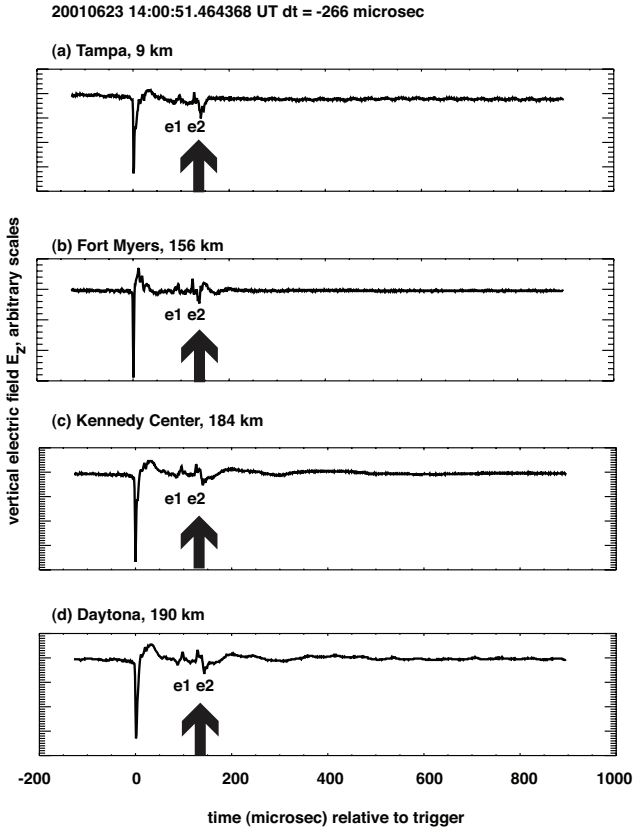

Fig. 4. Sferic electric field versus time for the four participating stations of one of the tightly-coincident sferics classified as an NBE (line #1 in Table 2). The arrows pointing at the second pulse are at the same time in each record. The "echoes" do not behave like ionospheric reflections, because they are roughly comparable in relative strength regardless of range, and because their delay (from the ground wave) is also independent of range. Apparently this sferic is actually due to a negative cloud-to-ground stroke, and the "echoes" are a detail of the groundwave.

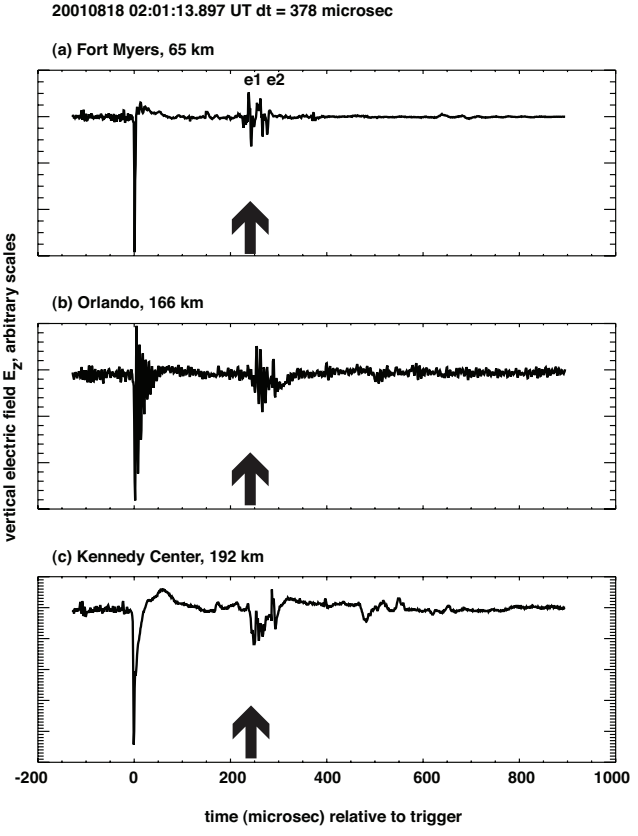

Fig. 5. Similar to Fig. 4, but for the coincidence in line #6 of Table 2. As in Fig. 4, the stroke automatically classified as an "NBE" is actually a negative cloud-to-ground stroke.

We see therefore that the five "NBEs" near the central correlation peak in Fig. 1 are all negative cloud-to-ground, not NBEs. The apparent NBE/photometer correlations were false. The four tight coincidences and the one nearly-tight coincidence originally classified as NBEs apparently leaked into the NBE class from the >50-fold more populous negative cloud-to-ground strokes. This corresponds to a small ($\sim$2 %) misclassification of negative cloud-to-ground strokes as negative NBEs. However, its effect is not small when attempting to assess the very small NBE correlation with the photometer trigger. Even the small ($\sim$2 %) missclassification (of negative cloud-to-ground strokes as negative NBEs) suffices to confound an initial look at whether a small number of NBEs are coincident with PDD activity.

As a control, we have checked the accuracy of the "null" NBEs, that is, the 149 NBEs that lacked any PDD concurrence within $\pm$10 ms (see Table 1). We find that three of these "null" NBEs are actually negative cloud-to-ground strokes, but that they were mistakenly classified as NBEs.

We conclude, therefore, that the original four (4) tightly-coincident NBEs in Table 1 must be corrected to zero (0). This correction is reflected in the last two rows of Table 1. The corrected conclusion is as follows: *In the context of the detection threshold of the PDD in nighttime operation, there is not even a single case of an NBE being tightly-coincident with a PDD trigger*. This is not to say that there can not be looser coincidences, beyond the central correlation peak of Fig. 1. However, those loose coincidences, even if above the level of statistical noise, would not be due to light directly emitted by the NBE event, but rather would be due to light emitted by either a preceding or a succeeding discharge event, outside the central peak of Fig. 1. The inference that NBEs are "dark" (relative to the PDD threshold), based on circumstantial evidence in an earlier study (Light and Jacobson, 2002), now has been confirmed by a direct comparison between light and sferics. All these inferences are subject to the top-of-cloud ERP threshold of $\sim 3 \times 10^8$ W. If NBEs were accompanied by tightly-correlated light emissions with top-of-cloud ERP below this threshold, then they would appear "dark" to the PDD.

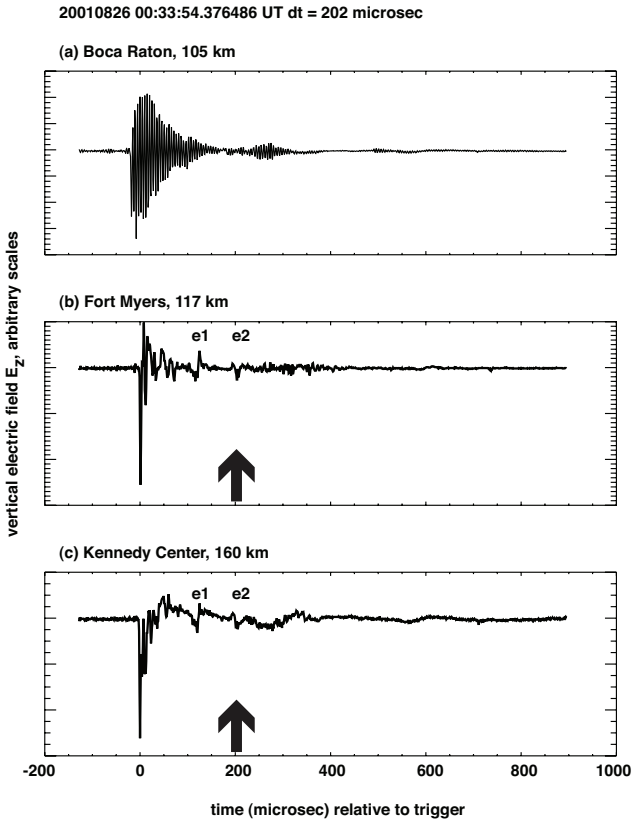

Fig. 6. Similar to Figs. 4 and 5, but for the coincidence in line #7 of Table 2. As in Figs. 4 and 5, the stroke automatically classified as an "NBE" is actually a negative cloud-to-ground stroke.

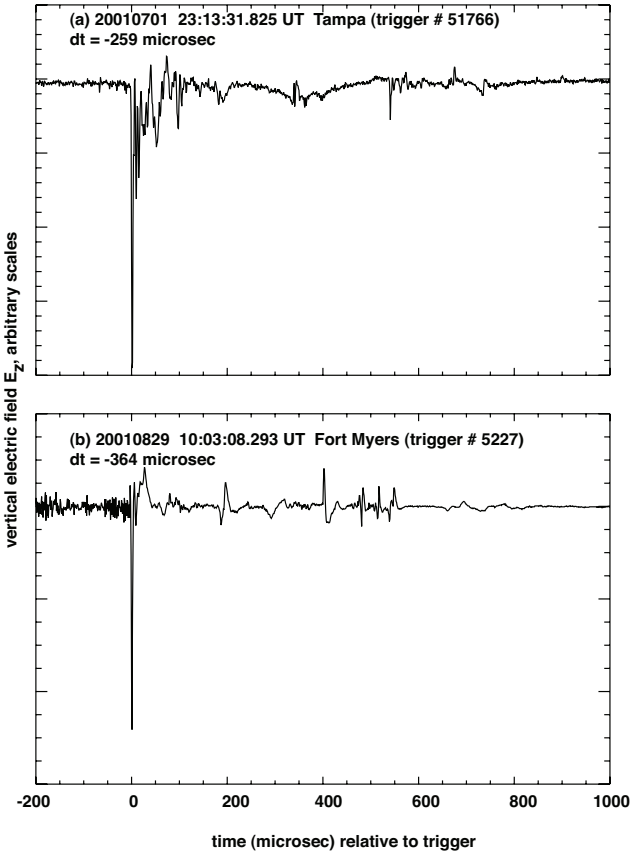

Fig. 7. Single-station sferic recordings for the two tightly-coincident cases lacking full multi-station waveforms. Their automated classification as "NBEs" is clearly erroneous; these are negative cloud-to-ground strokes. The precursor (leader) noise in **(b)** suggests that this stroke is the first stroke in its flash. See **(a)** Table 1, event 2, and **(b)** Table 1, event 8.

This conclusion must be qualified as follows. First, the satellite altitude is roughly 825 km, while the cloud top altitude can vary only within the upper troposphere, which is a small variation compared to the satellite altitude. The field-of-view of PDD is only $\sim \pm 40$ deg (Kirkland et al., 2001), so that the distance at the edge of the field-of-view does not exceed 150 % of the satellite altitude. Second, the cloud top behaves as the effective luminous source seen by the satellite. We shall assume that the cloud top-luminosity is isotropic, i.e., perfectly diffuse. The PDD trigger-level irradiance at the sensor was about $3 \times 10^{-5}\,\mathrm{W\,m^{-2}}$ (see Fig. 7 in Kirkland et al., 2001). A typical slant range from the sensor to the cloud top within the field-of-view is ∼900 km, implying that the optical ERP at the cloud top corresponding to the trigger threshold is $\sim 3 \times 10^8$ W. We do not know what the peak power is at the actual source within the cloud, other than that it is brighter; *all that matters is the cloud-top ERP* (Koshak et al., 1994; Light et al., 2001b). Relative to the trigger-threshold irradiance of $3 \times 10^{-5}\,\mathrm{W\,m^{-2}}$, PDD recorded a broad distribution of events distributed upward in irradiance to $> 3 \times 10^{-4}\,\mathrm{W\,m^{-2}}$ (Kirkland et al., 2001). Integrating over the pulse duration, the cloud-top Effective Radiated Energy was found to lie between $\sim 5 \times 10^4$ J and 1×10^6 J (see Fig. 8 in Kirkland et al., 2001). Typically the PDD recordings with trigger-threshold irradiance had implied cloud-top effective radiated energies in the range 5×10^4 J. By comparison, the original U-2 "groundtruth" reports of cloud-top effective radiated energies were between 10^5 to 10^6 J (Goodman et al., 1988). Thus by comparison with the U-2 observations, the NBE upper bound of $\sim 5 \times 10^4$ J cloud-top radiance is only one order-of-magnitude weaker than the ground-truthed radiances for ordinary lightning. This difference is *not* several orders-of-magnitude, and serves to temper any characterization of NBEs as "dark".

4 Comparison of sferic versus optical direct coincidence with FORTE VHF

The FORTE dual-channel VHF receiver always had at least one channel covering the "low band", 26–49 MHz. We use data from that low-band channel as the standard for comparing the radio power output of VHF emitters. Without

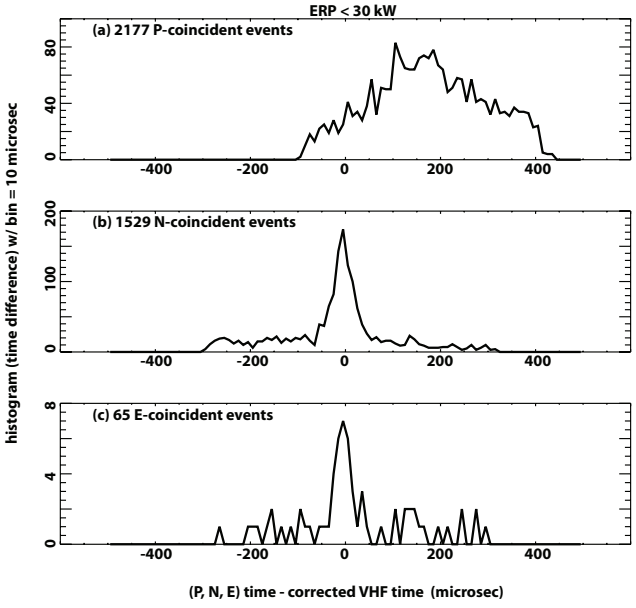

Fig. 8. Histograms of time differences between three coincidence-source trigger times, minus propagation-corrected FORTE VHF trigger times. VHF events are limited to the lowest-power: ERP <30 kW. Histogram uses a 10-μs bin. **(a)** Coincidence with combined optical photometer and imager triggers. **(b)** Coincidence with NLDN triggers. **(c)** Coincidence with LASA triggers.

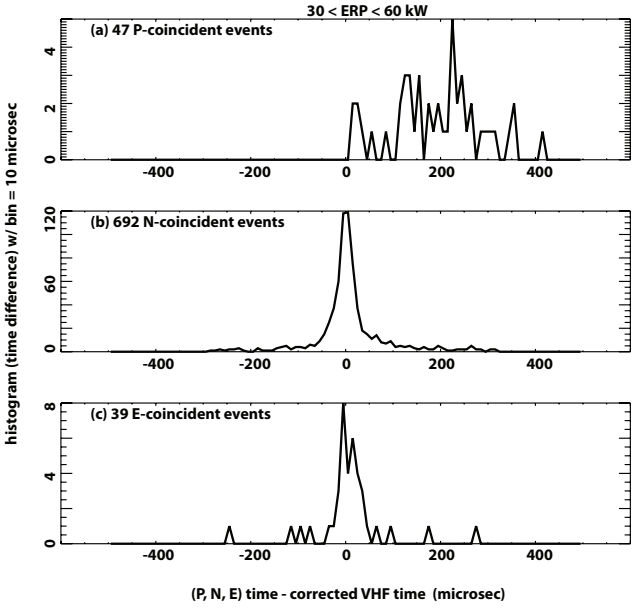

Fig. 9. Similar to Fig. 8, but for VHF events of mid-range power: $30 < \mathrm{ERP} < 60$ kW.

additional information, the FORTE VHF system on its own cannot precisely locate the source of the lightning, although some techniques can mitigate this uncertainty for certain emitters (Jacobson and Shao, 2001, 2002; Shao and Jacobson, 2002). When the VHF signal is closely coincident with other observations, such as, e.g., sferics or optical-imager detections, then the location of the source can be provided by the other observation, and the VHF detected peak power can be used to infer the source effective radiated power (ERP).

One advantage of VHF recordings from space is that it is frequently possible to reliably identify an intracloud emitter. This is because an emitted impulse of VHF has two paths to the satellite, the first being direct, and the second being downward to the reflective ground and thence (via reflection) up to the satellite (Holden et al., 1995; Jacobson et al., 1999, 2011; Massey and Holden, 1995; Massey et al., 1998a). The delayed arrival of the reflected pulse, with respect to the first, gives the impression of a "pulse pair". Further, the pulse is dispersed as one would expect for transmission through the ionosphere (Massey et al., 1998b). These pulse pairs are called "trans-ionospheric pulse pairs", or TIPPs, a moniker first used with the Blackbeard results on the Alexis satellite (Holden et al., 1995). If the horizontal position of the intracloud discharge is known (from, say, coincidence with other measurements), then the emission height can be inferred from the time splitting between the two pulses of the TIPP (Jacobson et al., 1999).

We reiterate that it is incorrect to label a radio-emission *process* as a "TIPP", because the phenomenon of a doubled pulse is *purely an artifact of the radiation's being observed from overhead*, i.e., from space. A ground-based observer of the same process would see a single pulse. Thus the moniker "TIPP" is meaningful only in the context of satellite VHF recordings.

In the remainder of this report, we focus exclusively on intracloud discharges recognized by their VHF TIPP structure. All the VHF data to follow are recognizable TIPPs meeting standard quality-control criteria (Jacobson et al., 1999).

We now compare the time coincidences of FORTE VHF TIPPs (a) with the LLS imager accompanied by the PDD photometer, (b) with NLDN, and (c) with LASA. The combination of the LLS/PDD joint detections is necessary because we want both good location accuracy (available from LLS, but not from PDD) and good temporal resolution (available from PDD, but not from LLS). We initially divide the VHF ERP into three gross ranges: <30 kW, 30–60 kW, and >60 kW. Figure 8 shows histograms of (a) PDD/LLS, or "P", corrected time differences from FORTE VHF triggers, (b) NLDN, or "N", corrected time differences from FORTE VHF triggers, and (c) LASA E-field, or "E", corrected time differences from FORTE VHF triggers. The bin size is 10 μs, and the distribution is plotted in the domain -500 to $+500$ μs. The VHF candidate events in Fig. 8 are only for ERP <30 kW, the lowest class of power. The optical correlations are collected anywhere on the FORTE orbit where both optical and VHF data are being simultaneously collected, whereas the NLDN correlations are limited to the CONUS, and the LASA correlations are limited to the

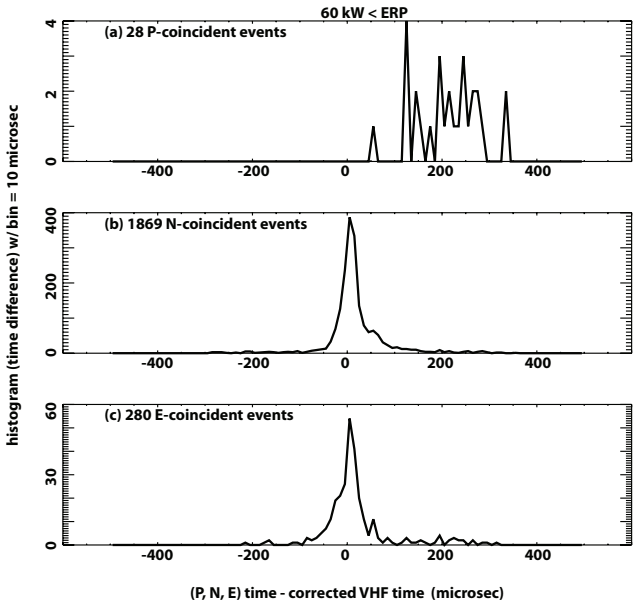

Fig. 10. Similar to Figs. 8 and 9, but for VHF events of highest power: 60 < ERP kW.

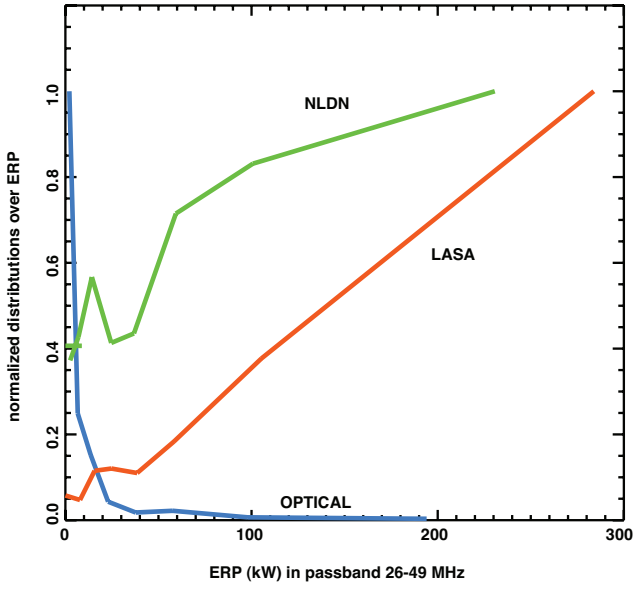

Fig. 11. Normalized distribution of the number of tight coincidences versus VHF ERP in the 26–49 MHz passband. Each data point's horizontal value is the median ERP within one of the eight bins of ERP of Table 3. The blue curve shows the normalized distribution of VHF ERP for optical coincidences with FORTE VHF. The NLDN coincidences are in green, and the LASA coincidences are in red. Each curve is separately normalized; see Table 3 for the unnormalized data in tabular form.

Florida area. Either of the two sferic correlations (b and c) show a narrow central peak surrounded by a noisy pedestal. The width of the central peak – a few tens' of microsec – is due to a combination of errors in the FORTE timing, errors in the FORTE ephemeris, and errors in the ionospheric correction for the VHF timing (Jacobson et al., 2000). Both the width and the gross delay of the optical correlation peak, on the other hand, are consistent with the original studies by other authors (Light and Hamlin, 2008; Suszcynsky et al., 2000). Those studies showed that most light emission *follows the associated VHF* (if there is associated VHF), and that the *light emission is extended over a much longer duration than is the associated VHF*. For satellite optical mapping of cloud-to-ground lightning, the light emission is preferentially due to delayed in-cloud disturbances even if the nominal "stroke" (and its closely tracking VHF) occur at or very near the ground.

Figure 9 is similar to Fig. 8, but for the mid-level ERP range: 30 to 60 kW. The LLS/PDD concurrence rate has collapsed relative to the sferic concurrence rate. The sferic concurrence histograms, for both NLDN and LASA, are more dominated by the central narrow peak, with less pedestal. This trend is continued in Fig. 10, for the highest level of ERP: >60 kW. Comparing Figs. 8, 9, and 10 we see that the *optical concurrence of VHF favors the lowest-ERP VHF emissions*, while the *sferic concurrence of VHF favors the highest-ERP VHF emissions*.

To study this trend with better energy resolution, we now divide ERP into eight narrower ranges, as shown in Table 3. For this display with finer ERP resolution, we do not need to resolve the time difference as well as in Figs. 8–10 above, so we include concurrence by LLS alone as a category of geolocation. The LLS time-stamps are not more precise than 2 ms, so they are not useful where fine time resolution is required. However, simply as a means of geolocating FORTE VHF emitters, the LLS time stamps are adequate, and significantly add to the number of geolocated events. In the following, we will combine the LLS-alone, and PDD-with-LLS coincidences together, in one category, "optical". Table 3 lists the matrix of VHF coincident transionospheric pulse pairs (TIPPs) for each source of concurrence and for each of the eight ranges of VHF ERP. Figure 11 illustrates the trends versus ERP, for each of the sources of concurrence: Optical (blue), NLDN (green), and LASA (red). Each curve is individually renormalized, for ease of comparing their trends versus ERP. The abscissa shows the median of the ERP within each ERP bin. Figure 11 shows clearly that optical concurrence drops sharply versus increasing VHF ERP, while sferic concurrence rises for the highest ERP. This serves to confirm the optical-concurrence trend identified in a previous study that was performed without source geolocation (Light and Jacobson, 2002). That study used VHF E^2 at the satellite, rather than VHF ERP at the source, to compare with rate of optical concurrence, and showed that for intracloud TIPPs, above a threshold of ERP, the trend of optical concurrence turned downward (see in particular Fig. 11 in Light and Jacobson, 2002).

Table 3. Number of TIPPs with given low-band (26–49 MHz) ERP and coincidence source (Optical, NLDN, and LASA). Total = 27 235 (unique: 21 874).

ERP range	Optical-coinc TIPPs	NLDN-coinc TIPPs	LASA-coinc TIPPs	Total coinc TIPPs
<5 kW	17 569	320	11	17 900
5–10 kW	2871	367	9	3247
10–20 kW	1400	487	22	1909
20–30 kW	407	355	23	785
30–45 kW	192	374	21	587
45–75 kW	147	614	35	796
75–140 kW	80	714	72	866
>140 kW	95	859	191	1145

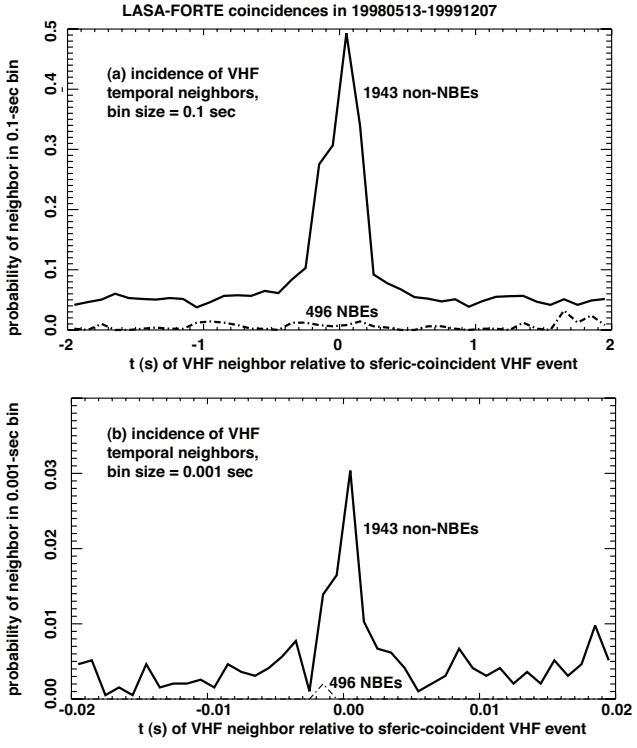

Fig. 12. Probability distribution of there being a FORTE VHF neighbor in bins of delay with respect to those FORTE VHF key events that are tight coincidences with LASA sferics. Solid curve: Non-NBE key events; dashed curve: NBE key events. Bin width is **(a)** 0.1 s, and **(b)** 0.001 s.

Thus the results of Figs. 8–11 of the present study confirm that at the high VHF TIPP ERP ranges, say >30 kW, the likelihood of prompt concurrence above the PDD threshold (top-of-cloud peak emission power $\sim 3 \times 10^8$ W) falls monotonically versus increasing ERP. We remark that since the earliest report of NBE sferics (Le Vine, 1980), all studies of this phenomenon have observed that NBE sferics are synchronously accompanied by the most intense VHF emissions of any lightning (Jacobson et al., 1999, 2000; Jacobson and Light, 2003; Nag and Rakov, 2009, 2010a, b; Nag et al., 2010; Smith, 1998; Smith et al., 1999; Thomas et al., 2001; Willett et al., 1989, 1990; Willett and Krider, 2000). Thus, the results of Figs. 8–11 of the present study also implicitly corroborate the association of NBE sferics with suppressed optical emissions; see Sect. 3 above for a more direct test of that association.

5 Probability of flash neighbors of FORTE VHF TIPPs

We now examine the ERP dependence of the probability of VHF TIPPs' being clustered-together in time, versus being isolated. In early reports of the NBE sferic accompanied by intense high-frequency noise (Le Vine, 1980; Willett et al., 1989), it was observed that NBEs tend to occur in temporal isolation from other lightning processes. However, Lightning Mapper Array (LMA) observations have been reported to implicate some extremely intense VHF intracloud emissions as marking the initiation of at least certain intracloud flashes (Rison et al., 1999; Thomas et al., 2001). A report based on FORTE observations (Jacobson, 2003b) tended to corroborate the LMA observations. In this section, we extend the FORTE-based observations to increase their statistical significance.

We begin with the simple case of comparing VHF recordings that are coincident with LASA NBEs, compared to those which are coincident with LASA non-NBEs. For this particular application we are using both TIPPs and non-TIPPs in the VHF archive. For each case we then compute the probability that a LASA-coincident VHF event, considered as a "key" event, will have temporally neighboring VHF events.

Figure 12 shows the observed probability of there being a neighboring event in a delay bin, for (a) binwidth = 100 ms, and (b) binwidth = 1 ms. The LASA locations may be at all ranges, not just within 400 km of the array center, for Fig. 12. The solid curve is for VHF key events which are tightly coincident with LASA non-NBE sferics, while the dashed curve is for VHF key events which are tightly coincident

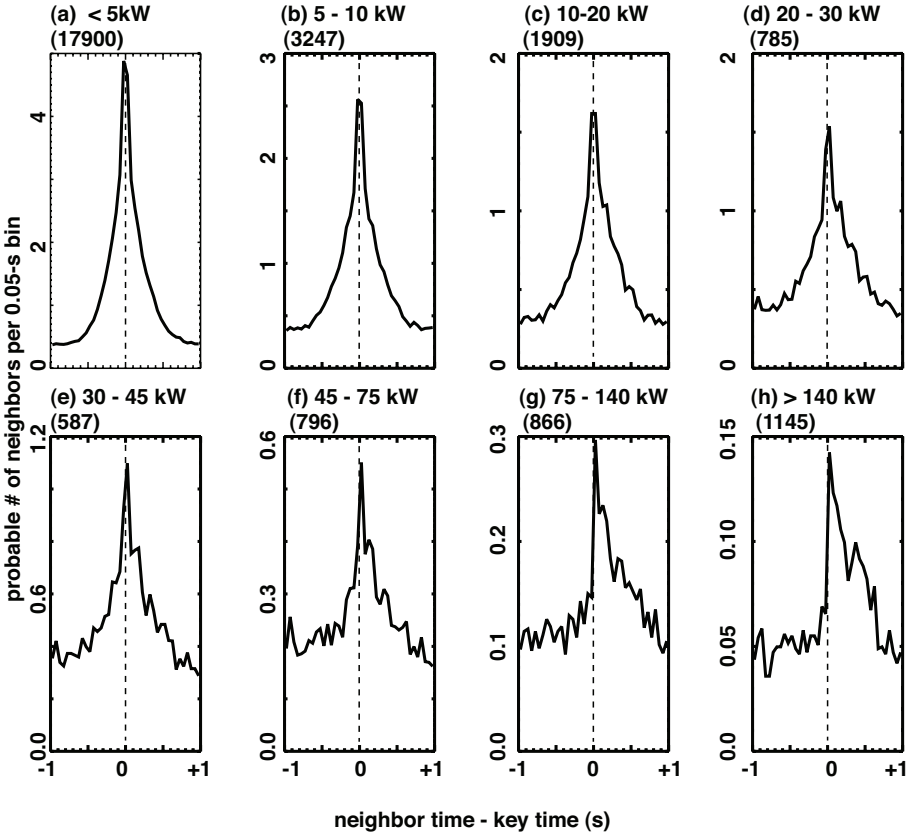

Fig. 13. Probability distribution of there being a FORTE VHF neighbor in bins of delay with respect to FORTE VHF key events coincident with any of the coincidence systems in Table 3. These key events are stratified by their ERP into eight ranges, from **(a)** ERP < 5 kW, through **(h)** ERP > 140 kW. The bin width is 0.05 s.

with LASA NBE sferics. For this limited dataset that has LASA ground-truth on whether the coincidence is from an NBE, it appears that NBE-coincident VHF events show no significant pattern of proximity to flash neighbors, unlike the non-NBE-coincident VHF events. This would tend to agree with the earliest, pre-LMA reports (Le Vine, 1980; Willett et al., 1989).

Next, we take directly-geolocated intracloud TIPPs with any form of coincidence (L, P, N, E; see Table 3) and study their temporal proximity to other TIPPs after stratifying by ERP. Figure 13 shows the probability of there being TIPP neighbors in bins of 50-ms width, in each of the eight classes of ERP shown in Table 3. The neighbors are included only if their slant total electron content, or TEC, is within $\pm 10^{17}\,\mathrm{m}^{-2}$ of the key event's TEC. This requirement provides some rudimentary protection against mixing events of unrelated (spatially separated) storms. Figure 13 shows the progression of neighbor probability vs. time separation, from a symmetric, (a) high probability at low key-event ERP, to (h) an asymmetric, low probability at the highest key-event ERP. The sign of the asymmetry for high key-event ERP is that those key events have extra neighbors after the key event, but not before the key event. This behavior is akin to what was noted in LMA studies earlier (Rison et al., 1999; Thomas et al., 2001). We caution, however, that the probability of post-key-event neighbors of key events with high ERP is still rather low, even if it is higher than the probability of pre-key-event neighbors. For example, in Fig. 13h, the post-key-event enhancement averages about 0.05 neighbors per 50-ms bin, over about eight such bins (0.4 s). This means that the probable number of flash-associated neighbors (above the statistical background) is only 0.4, following a key event in the ERP > 140 kW. That is hardly a populous intracloud flash.

6 Conclusions

(a) We have catalogued 10 061 lightning strokes detected, located and classified by LASA and occuring during instantaneous visibility to the FORTE satellite's non-imaging photometer in nighttime operation. These 10 061 LASA strokes have then been divided into NBE versus non-NBE classification, and within each of those classifications, split into either coincident, or non-coincident, with photometer triggers. The photometer trigger level corresponds to $\sim 3 \times 10^8$ W

of optical effective isotropic power at the top of the cloud. We show that 154 of the 10 061 events are classified as NBEs, while the rest are non-NBEs. Of the non-NBEs, 1161 ($\sim$12 %) are accompanied by coincident photometer triggers. On the other hand, of the 154 NBEs (excluding five false classifications), none (0 %) is accompanied by tight-coincident photometer triggers. Thus we conclude that the none of the 154 NBEs was capable of producing 3×10^8 W of optical effective isotropic power at the top of the cloud.

(b) To perform a related test of the probability of VHF TIPPs to be accompanied by light above the photometer threshold, we have stratified 21 874 unique, coincidence-located TIPPs into eight classes of VHF ERP in the 26–49 MHz passband. For each class of ERP, we tally the numbers of TIPPs whose concurrence is by the photometer, by the optical imager aboard FORTE, by LASA, or by NLDN. We find that for TIPPs concurrent with sferics, the distribution rises with increasing VHF ERP, while for TIPPs concurrent with optical, the distribution falls monotonically versus ERP, reaching a statistically negligible level at the highest ERP. This test is a complement to the first test above.

(c) Using the same stratification of the 21 874 coincidence-locatd VHF TIPPs by their ERP, we have tested for the proximity of temporally neighboring VHF events (of any ERP). We find that the probability of neighbors within ± 0.5 s is statistically negligible for the highest ERP class ($>$140 kW), but increases monotonically as ERP decreases.

Acknowledgements. A. R. Jacobson has been supported in this work by a grant from the Defense Advanced Research Projects Agency's NIMBUS program, led by M. Goodman.

T. E. L. Light has participated under the auspices of the United States Department of Energy.

None of this work would have been possible without the diligent support of the FORTE flight-operations team, led by Diane Rousselle-Dupré and Phillip Klingner. Nor would this work have been possible without the design, construction, tending, and maintenance of LASA by the LASA team, including Robert Massey (deceased), David A. Smith, Mathew Heavner, Jeremiah Harlin, and Ken Eack.

Topical Editor P. Drobinski thanks two anonymous referees for their help in evaluating this paper.

References

Boccippio, D. J., Driscoll, K., Koshak, W., Blakeslee, R., Boeck, W., Buechler, D., Christian, H., and Goodman, S.: The Optical Transient Detector (OTD): Instrument characteristics and cross-sensor validation, J. Atmos. Oceanic Tech., 17, 441–458, 2000.

Christian, H. J., Blakeslee, R. J., Goodman, S. J., Mach, D. A., Stewart, M. F., Buechler, D. E., Koshak, W. J., Hall, J. M., Boeck, W. L., Driscoll, K. T., and Boccippio, D. J.: The Lightning Imaging Sensor, paper presented at 11th International Conference on Atmospheric Electricity, NASA, Global Hydrology and Climate Center, NASA Marshall Space Flight Center, Huntsville, Alabama, 1999.

Christian, H. J., Blakeslee, R. J., Boccippio, D. J., Boeck, W. L., Buechler, D. E., Driscoll, K. T., Goodman, S. J., Hall, J. M., Koshak, W. J., Mach, D. M., and Stewart, M. F.: Global frequency and distribution of lightning as observed from space by the Optical Transient Detector, J. Geophys. Res., 108, 4005, doi:10.1029/2002JD002347, 2003.

Cummins, K. L. and Murphy, M. J.: An overview of lightning location systems: History, techniques, and data uses, with an in-depth look at the U. S. NLDN, IEEE Trans. Electromagnetic Compatibility, 51, 499–518, 2009.

Cummins, K. L., Murphy, M. J., Bardo, E. A., Hiscox, W. L., Pyle, R., and Pifer, A. E.: Combined TOA/MDF technology upgrade of U. S. National Lightning Detection Network, J. Geophys. Res., 103, 9035–9044, 1998.

Davis, S. M., Suszcynsky, D. M., and Light, T. E. L.: FORTE observations of optical emissions from lightning: Optical properties and discrimination capability, J. Geophys. Res., 107, 4579, doi:10.1029/2002JD002434, 2002.

Dwyer, J. R.: Source mechanisms of terrestrial gamma-ray flashes, J. Geophys. Res., 113, D10103, doi:10.1029/2007JD009248, 2008.

Goodman, S. J., Christian, H. J., and Rust, W. D.: A comparison of the optical pulse characteristics of intracloud and cloud-to-ground lightning as observed above clouds, J. Appl. Meteor., 27, 1369–1381, 1988.

Grefenstette, B. W., Smith, D. M., Dwyer, J. R., and Fishman, G. J.: Time evolution of terrestrial gamma ray flashes, Geophys. Res. Lett., 35, L06802, doi:10.1029/2007GL032922, 2008.

Grefenstette, B. W., Smith, D. M., Hazelton, B. J., and Lopez, L. I.: First RHESSI terrestrial gamma ray flash catalogue, J. Geophys. Res., 114, A02314, doi:10.1029/2008JA013721, 2009.

Heavner, M. J., Smith, D. A., Jacobson, A. R., and Sheldon, R. J.: LF/VLF and VHF lightning fast-stepped leader observations, J. Geophys. Res., 107, 4791, doi:10.1029/2001JD001290, 2002.

Holden, D. N., Munson, C. P., and Devenport, J. C.: Satellite observations of transionospheric pulse pairs, Geophys. Res. Lett., 22, 889–892, 1995.

Jacobson, A. R.: Relationship of intracloud-lightning radiofrequency power to lightning-storm height, as observed by the FORTE satellite, J. Geophys. Res., 108, 4204, doi:1029/2002JD002956, 2003a.

Jacobson, A. R.: How do the strongest radio pulses from thunderstorms relate to lightning flashes?, J. Geophys. Res., 108, 4778, doi:10.1029/2003JD003936, 2003b.

Jacobson, A. R. and Heavner, M. J.: Comparison of Narrow Bipolar Events with ordinary lightning as proxies for severe convection, Mon. Weather Rev., 133, 1144–1154, 2005.

Jacobson, A. R. and Light, T. E. L.: Bimodal radiofrequency pulse distribution of intracloud-lightning signals recorded by the FORTE satellite, J. Geophys. Res., 108, 4266, doi:10.1029/2002JD002613, 2003.

Jacobson, A. R. and Shao, X.-M.: Using geomagnetic birefringence to locate sources of impulsive, terrestrial VHF signals detected by satellites on orbit, Radio Sci., 36, 671–680, 2001.

Jacobson, A. R. and Shao, X.-M.: On-orbit direction-finding of lightning radio-frequency emissions recorded by the FORTE satellite, Radio Sci., 37, doi:10.1029/2001RS002510, 2002.

Jacobson, A. R., Knox, S. O., Franz, R., and Enemark, D. C.: FORTE observations of lightning radio-frequency signatures: Capabilities and basic results, Radio Sci., 34, 337–354, 1999.

Jacobson, A. R., Cummins, K. L., Carter, M., Klingner, P., Roussel-

Dupré, D., and Knox, S. O.: FORTE radio-frequency observations of lightning strokes detected by the National Lightning Detection Network, J. Geophys. Res., 105, 15653–15662, 2000.

Jacobson, A. R., Boeck, W., and Jeffery, C.: Comparison of Narrow Bipolar Events with ordinary lightning as proxies for the microwave-radiometry ice-scattering signature, Mon. Weather Rev., 135, 1354–1363, 2007.

Jacobson, A. R., Holzworth, R. H., and Shao, X.-M.: Observations of multi-microsecond VHF pulsetrains in energetic intracloud lightning discharges, Ann. Geophys., 29, 1587–1604, doi:10.5194/angeo-29-1587-2011, 2011.

Kirkland, M. W., Suszcynsky, D. M., Guillen, J. L. L., and Green, J. L.: Optical observations of terrestrial lightning by the FORTE satellite photodiode detector, J. Geophys. Res., 106, 33499–33509, 2001.

Kitagawa, T. and Brook, M.: A comparison of intracloud and cloud-to-ground lightning discharges, J. Geophys. Res., 65, 1189–1201, 1960.

Koshak, W. J., Solakiewicz, R. J., Phanord, D. D., and Blakeslee, R. J.: Diffusion model for lightning radiative transfer, J. Geophys. Res., 99, 14361–14371, 1994.

Lay, E. H. and Shao, X.-M.: High temporal and spatial-resolution detection of D-layer fluctuations by using time-domain lightning waveforms, J. Geophys. Res., 116, A01317, doi:10.1029/2010JA016018, 2011.

Le Vine, D. M.:, Sources of the strongest rf radiation from lightning, J. Geophys. Res., 85, 4091–4095, 1980.

Light, T. E. L. and Jacobson, A. R.: Characteristics of impulsive VHF lightning observed by the FORTE satellite, J. Geophys. Res., 107, 4756, doi:1029/2001/JD001585, 2002.

Light, T. and Hamlin, T.: Coordinated Optical/VLF Lightning Observations, Eos Trans. AGU, 89(53 Fall Meeting Supplement), AE11A-0293, 2008.

Light, T. E., Suszcynsky, D. M., and Jacobson, A. R.: Coincident Radio Frequency and Optical Emissions from Lightning, Observed with the FORTE Satellite, J. Geophys. Res., 106, 28223–28231, 2001a.

Light, T. E., Suszcynsky, D. M., Kirkland, M. W., and Jacobson, A. R.: Simulations of lightning optical waveforms as seen through clouds by satellites, J. Geophys. Res., 106, 17103–17114, 2001b.

Massey, R. S. and Holden, D. N.: Phenomenology of transionospheric pulse pairs, Radio Sci., 30, 1645–1659, 1995.

Massey, R. S., Holden, D. N., and Shao, X.-M.: Phenomenology of trans-ionospheric pulse pairs: Further observations, Radio Sci., 33, 1755–1761, 1998a.

Massey, R. S., Knox, S. O., Franz, R. C., Holden, D. N., and Rhodes, C. T.: Measurements of transionospheric radio propagation parameters using the FORTE satellite, Radio Sci., 33, 1739–1753, 1998b.

Massey, R. S., Eack, K. B., Eberle, M. H., Shao, X. M., Smith, D. A., and Wiens, K. C.: Operation of an array of field-change detectors to provide ground truth for FORTE data, in: Proceedings of the 11th International Conference on Atmospheric Electricity, paper presented at 11th International Conference on Atmospheric Electricity, International Commission on Atmospheric Electricity, Global Hydrology and Climate Center, NASA Marshall Space Flight Center, Huntsville, Alabama, 1999.

Nag, A. and Rakov, V. A.: Electromagnetic pulses produced by bouncing-wave-type lightning discharges, IEEE Trans. Electromagnetic Compatibility, 51, 466–470, 2009.

Nag, A. and Rakov, V. A.: Compact intracloud lightning discharges: 1. Mechanism of electromagnetic radiation and modeling, J. Geophys. Res., 115, D20102, doi:1029/2010JD014235, 2010a.

Nag, A. and Rakov, V. A.: Compact intracloud lightning discharges: 2. Estimation of electrical parameters, J. Geophys. Res., 115, D20103, doi:10.1029/2010JD014237, 2010b.

Nag, A., Rakov, V. A., Tsalikis, D., and Cramer, J. A.: On phenomenology of compact intracloud lightning discharges, J. Geophys. Res., 115, D14115, doi:10.1029/2009JD012957, 2010.

Rison, W., Thomas, R. J., Krehbiel, P. R., Hamlin, T., and Harlin, J.: A GPS-based three-dimensional lightning mapping system: Initial observations in central New Mexico, Geophys. Res. Lett., 26, 3573–3576, 1999.

Shao, X.-M. and Jacobson, A. R.: Polarization observations of broadband VHF signals by the FORTE satellite, Radio Sci., 36, 1573–1589, 2001.

Shao, X.-M. and Jacobson, A. R.: Polarization observations of lightning-produced VHF emissions by the FORTE satellite, J. Geophys. Res., 107, 4430, doi:10.1029/2001JD001018, 2002.

Shao, X., Jacobson, A. R., and Fitzgerald, T. J.: Radio frequency radiation beam pattern of lightning return strokes: A revisit to theoretical analysis, J. Geophys. Res., 109, D19108, doi:10.1029/2004JD004612, 2004.

Shao, X.-M., Jacobson, A. R., and Fitzgerald, T. J.: Radio frequency radiation beam pattern of lightning return strokes: Inferred from FORTE satellite observations, J. Geophys. Res., 110, D24102, doi:10.1029/2005JD006010, 2005.

Smith, D. A.: Compact intracloud discharges, PhD thesis, 272 pp., University of Colorado, Boulder, CO, 1998.

Smith, D. A., Shao, X. M., Holden, D. N., Rhodes, C. T., Brook, M., Krehbiel, P. R., Stanley, M., Rison, W., and Thomas, R. J.: A distinct class of isolated intracloud lightning discharges and their associated radio emissions, J. Geophys. Res., 104, 4189–4212, 1999.

Smith, D. A., Eack, K. B., Harlin, J., Heavner, M. J., Jacobson, A. R., Massey, R. S., Shao, X. M., and Wiens, K. C.: The Los Alamos Sferic Array: A research tool for lightning investigations, J. Geophys. Res., 107, 4183, doi:10.1029/2001JD000502, 2002.

Smith, D. A., Heavner, M. J., Jacobson, A. R., Shao, X. M., Massey, R. S., Sheldon, R. J., and Wiens, K. C.: A method for determining intracloud lightning and ionospheric heights from VLF/LF electric field records, Radio Sci., 39, RS1010, doi:10.1029/2002RS002790, 2004.

Suszcynsky, D. M. and Heavner, M. J.: Narrow Bipolar Events as indicators of thunderstorm convective strength, Geophys. Res. Lett., 30, 1879, doi:10.1029/2003GL017834, 2003.

Suszcynsky, D. M., Kirkland, M. W., Jacobson, A. R., Franz, R. C., Knox, S. O., Guillen, J. L. L., and Green, J. L.: FORTE observations of simultaneous VHF and optical emissions from lightning: Basic Phenomenology, J. Geophys. Res., 105, 2191–2201, 2000.

Suszcynsky, D. M., Light, T. E., Davis, S., Kirkland, M. W., Green, J. L., and Guillen, J.: Coordinated Observations of Optical Lightning from Space using the FORTE Photodiode Detector and CCD Imager, J. Geophys. Res., 106, 17897–17906, 2001.

Thomas, R. J., Krehbiel, P. R., Rison, W., Hamlin, T., Harlin, J., and Shown, D.: Observations of VHF source powers radiated by

lightning, Geophys. Res. Lett., 28, 143–146, 2001.

Tierney, H. E., Jacobson, A. R., Roussel-Dupré, R., and Beasley, W. H.: Transionospheric pulse pairs originating in marine, continental and coastal thunderstorms: Pulse energy ratios, Radio Sci., 37, 11-11–11-17, 2002.

Wiens, K. C., Hamlin, T. D., Harlin, J., and Suszcynsky, D.: Relationships among Narrow Bipolar Events, "total" lightning, and radar-inferred convective strength in Great Plains Thunderstorms, J. Geophys. Res., 113, D05201, doi:10.1029/2007JD009400, 2008.

Willett, J. C. and Krider, E. P.: Rise times of impulsive high-current processes in cloud-to-ground lightning, IEEE Trans. Ant. Prop., 48, 1442–1451, 2000.

Willett, J. C., Bailey, J. C., and Krider, E. P.: A class of unusual lightning electric field waveforms with very strong high-frequency radiation, J. Geophys. Res., 94, 16255–16267, 1989.

Willett, J. C., Bailey, J. C., Leteinturier, C., and Krider, E. P.: Lightning electromagnetic radiation field spectra in the interval from 0.2 to 20 MHz, J. Geophys. Res., 95, 20367–20387, 1990.

Willett, J. C., Krider, E. P., and Leteinturier, C.: Submicrosecond field variations during the onset of first return strokes in cloud-to-ground lightning, J. Geophys. Res., 103, 9027–9034, 1998.

Wu, T., Dong, W., Zhang, Y., and Wang, T.: Comparison of positive and negative compact intracloud discharges, J. Geophys. Res., 116, D03111, doi:10.1029/2010JD015233, 2011.

Zuelsdorf, R. S., Strangeway, R. J., Russell, C. T., Casler, C., Christian, H. J., and Franz, R. C.: Transionospheric pulse pairs (TIPPs): Their geographic distributions and seasonal variations, Geophys. Res. Lett., 24, 3165–3168, 1997.

Zuelsdorf, R. S., Casler, C., Strangeway, R. J., Russell, C. T., and Franz, R. C.: Ground detection of trans-ionospheric pulsed pairs by stations in the National Lightning Detection Network, Geophys. Res. Lett., 25, 481–484, 1998.